ELSEVIER

Adaptive Nonlinear Optimal Compensation Control for Electro-hydraulic Load Simulator

Yao Jianyong, Jiao Zongxia*, Shang Yaoxing, Huang Cheng

National Key Laboratory of Science and Technology on Holistic Control, Beijing University of Aeronautics and Astronautics, Beijing 100191, China

Abstract

Directing to the strong position coupling problem of electro-hydraulic load simulator (EHLS), this article presents an adaptive nonlinear optimal compensation control strategy based on two estimated nonlinear parameters, viz. the flow gain coefficient of servo valve and total factors of flow-pressure coefficient. Taking trace error of torque control system to zero as control object, this article designs the adaptive nonlinear optimal compensation control strategy, which regards torque control output of closed-loop controller converging to zero as the control target, to optimize torque tracking performance. Electro-hydraulic load simulator is a typical case of the torque system which is strongly coupled with a hydraulic positioning system. This article firstly builds and analyzes the mathematical models of hydraulic torque and positioning system, then designs an adaptive nonlinear optimal compensation controller, proves the validity of parameters estimation, and shows the comparison data among three control structures with various typical operating conditions, including proportion-integral-derivative (PID) controller only, the velocity synchronizing controller plus PID controller and the proposed adaptive nonlinear optimal compensation controller plus PID controller. Experimental results show that systems' nonlinear parameters are estimated exactly using the proposed method, and the trace accuracy of the torque system is greatly enhanced by adaptive nonlinear optimal compensation control, and the torque servo system capability against sudden disturbance can be greatly improved.

Keywords: torque control; nonlinear control; optimal control; adaptive; electro-hydraulic load simulator; parameter estimation; position disturbance

1. Introduction

Electro-hydraulic load simulator (EHLS), also named loading system, is a widely used hardware-in-loop-simulation assembly in flight control system development [1-2], which could simulate the air load executed in positioning actuator system. Due to the direct connection between EHLS and the positioning actuator system, the operation of actuator leads to heavy disturbance to EHLS which is called extraneous force/torque [2]. Therefore EHLS is a typical electro-hydraulic force/torque system strongly coupled with motion disturbance. How to eliminate the extraneous force/torque becomes a hotspot in EHLS, and we could divide the relevant literature into two types.

(1) The displacement/velocity synchronization

The idea of the displacement/velocity synchronization is to let EHLS track the operation of actuator system and execute the load on it. In this area, C. Y. Yu, et al. utilized an accessional hydraulic motor to keep the EHLS synchronization to the actuation so as to reduce the extraneous torque [3]. Q. Hua and Z. X. Jiao, et al. investigated the disturbance root of EHLS and presented a velocity synchronous control method through importing the control output of actuator system [1,4], in which the advance compensation is carried out to decrease the external disturbance. Based on the above idea, there are lots of research works laying emphasis on velocity forward compensation to eliminate the extraneous torque [5-6]. A. R. Plummer brought forward a cross compensation method to improve force trace accuracy whose essence was also velocity synchronization [7].

(2) Anti-disturbance control

Taking the displacement coupling as a disturbance, the second type adopted the robust EHLS to improve its anti-disturbance capability. In this area, D. Q. Truong, et al. proposed a fuzzy proportion-integral-derivative (PID) with a self-tuning grey predictor to improve the robustness against external disturbances [8]. A robust force controller through an inverse

dynamic model of the actuator was described in Ref.[9], which was insensitive to the load dynamics. N. Yoonsu designed a robust control method based on quantitative feedback theory (QFT) to enhance the EHLS robustness[10-11]. F. C. Mare investigated a hybrid control scheme including compensation of load velocity, torque input feed-forward and PID control for high speed aerospace actuator[12]. S. Chantranuwathana, et al. presented the modular adaptive robust control (MARC) technique to improve the force control performance of vehicle active suspensions[13]. Afterward, many nonlinear control methods such as neural network and optimization were widely utilized in EHLS[14-16]. An optimal-tuning nonlinear PID control of hydraulic systems had also been proposed by G. P. Liu, et al.[17-18]. R. D. Abbott, et al. gave an optimal control synthesis strategy to an electro-hydraulic positioning system[19].

This article proposes an adaptive nonlinear optimal compensation control strategy, which takes the minimum of the control output of force/torque closed-loop controller as optimal compensation objective other than the synchronous control and anti-disturbance control aforementioned. It is a novel control scheme, which does not take actuator's motion as disturbance, but designs an adaptive nonlinear optimal compensation controller aimed at minimizing the torque trace error.

The article is organized as follows. Section 2 formulates and analyzes the system mathematic models. And the controller design method of the adaptive nonlinear optimal compensation is applied in Section 3. An electro-hydraulic load simulator is used as a case study in Section 4, including validity demonstration and detail comparison of three types of control strategies under various working conditions. Conclusions are to be found in Section 5.

2. Mathematic Models of EHLS and Positioning Actuator System

The structure of electro-hydraulic load simulator and positioning actuator system is shown in Fig.1.
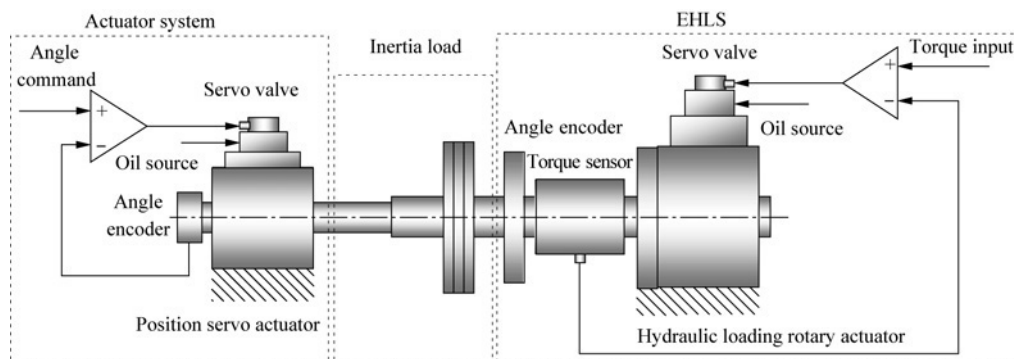

Fig.1   Architecture of electro-hydraulic load simulator.

The left part in Fig.1 is actuator system, which is consisted of hydraulic servo valve, position servo actuator and angle encoder. EHLS is on the right side that consists of hydraulic loading rotary actuator, servo valve, torque sensor, inertia load and angle encoder. It is obvious that EHLS could output extraneous torque without any command when the actuator system operates. So the EHLS and actuator system exist inherent coupling and interacting. The torque output of EHLS is a strong disturbance for motion control of actuator system. At the same time, the motion of actuator is also a strong disturbance for EHLS torque control. Motion disturbance is the main problem in EHLS.

In order to describe the relationship of EHLS and actuator system, their mathematic model is established as follows.

Notations in the equations of Section 2.1 and Section 2.2 are as follows:

ω—Angle velocity of actuator, rad/s;

θ_m—Angle output of actuator system, rad;

B_L—Viscous damping of loading system, N·m·s/rad;

B_m—Viscous damping of actuator system, N·m·s/rad;

C_{sl}—Leakage coefficient of actuator, m⁵/(N·s);

C_{slL}—Leakage coefficient of loading hydraulic rotary actuator, m⁵/(N·s);

C_v—Flow coefficient of orifice of actuator system;

C_{vL}—Flow coefficient of orifice of loading system;

D_L—Radian displacement of loading hydraulic rotary actuator, m³/rad;

D_m—Radian displacement of actuator, m³/rad;

J_L—Rotor inertia of loading system, kg·m²;

J_m—Rotor inertia of actuator system, kg·m²;

K_c—Coefficient of flow rate to pressure of actuator servo valve, m⁵/(N·s);

K_{cL}—Coefficient of flow rate to pressure of loading servo valve, m⁵/(N·s);

K_Q—Flow rate gain of actuator servo valve, m²/s;

K_{QL}—Flow rate gain of loading servo valve, m²/s;

K_{tmL}—Total factor of flow rate to pressure of loading system, m⁵/(N·s);

K_{tm}—Total factor of flow rate to pressure of actuator system, m⁵/(N·s);

p_{fL}—Load pressure of loading system, N/m²;

p_f—Load pressure of actuator system, N/m^2;

p_s—Oil source pressure of actuator system, N/m^2;

p_{sL}—Oil source pressure of loading system, N/m^2;

Q_f—Load flow rate of actuator system, m^3/s;

Q_{fL}—Load flow rate of loading system, m^3/s;

s —Differential operator.

sign(·)—Function of sign;

T_L—Output of loading system, N·m;

W—Area gradient of actuator servo valve, m;

W_L—Area gradient of loading servo valve, m;

x_v—Servo valve spool displacement of actuator system, m;

x_{vL}—Servo valve spool displacement of loading system, m;

ρ —Density of hydraulic oil, kg/m^3.

2.1. Mathematic model of actuator system

The dynamics characteristics of the actuator system are described by the following equations.

(1) Flow equation of servo valve

Eq.(1) is the orifice equation of the servo valve, in which the leakage is neglected.

$$Q_f = C_v W x_v \sqrt{\frac{1}{\rho}(p_s - \mathrm{sign}(x_v)p_f)} \qquad (1)$$

The orifice equation can be linearized as

$$Q_f = K_Q x_v - K_c p_f \qquad (2)$$

where

$$K_Q = C_v W \sqrt{\frac{1}{\rho}(p_s - \mathrm{sign}(x_v)p_f)} \qquad (3)$$

$$K_c = \frac{1}{2} C_v W |x_v| \sqrt{\frac{1}{\rho(p_s - \mathrm{sign}(x_v)p_f)}} \qquad (4)$$

(2) The load flow continuity equation is Eq.(5), where the compressibility of hydraulic oil is neglected.

$$Q_f = D_m \omega + C_{sl} p_f \qquad (5)$$

(3) Motion equation

$$D_m p_f + T_L = J_m \omega s + B_m \omega \qquad (6)$$

Combining Eqs.(2)-(5) with Eq.(6) gives the mathematical model of positioning actuator system:

$$\theta_m(s) = \frac{1}{s}\omega = \left[\frac{D_m K_Q}{K_{tm}} x_v + T_L(s)\right] \Bigg/ \left[\left(J_m s + B_m + \frac{D_m^2}{K_{tm}}\right)s\right] \qquad (7)$$

where

$$K_{tm} = K_c + C_{sl} \qquad (8)$$

2.2. Mathematic model of EHLS

(1) The orifice equation of the servo valve is

$$Q_{fL} = C_{vL} W_L x_{vL} \sqrt{\frac{1}{\rho}(p_{sL} - \mathrm{sign}(x_{vL})p_{fL})} \qquad (9)$$

Linearize it in operation point as

$$Q_{fL} = K_{QL} x_{vL} - K_{cL} p_{fL} \qquad (10)$$

where

$$K_{QL} = C_{vL} W_L \sqrt{\frac{1}{\rho}(p_{sL} - \mathrm{sign}(x_{vL})p_{fL})} \qquad (11)$$

$$K_{cL} = \frac{1}{2} C_{vL} W_L |x_{vL}| \sqrt{\frac{1}{\rho(p_{sL} - \mathrm{sign}(x_{vL})p_{fL})}} \qquad (12)$$

(2) The load flow continuity equation

$$Q_{fL} = D_L \omega + C_{slL} p_{fL} \qquad (13)$$

(3) Torque balance equation

$$D_L p_{fL} - T_L = J_L \omega s + B_L \omega \qquad (14)$$

Combining Eqs.(10)-(13) with Eq.(14) gives the mathematical model of EHLS:

$$T_L(s) = \frac{K_{QL} D_L}{K_{tmL}} x_{vL} - (J_L s + B_L + \frac{D_L^2}{K_{tmL}})s\theta_m(s) \qquad (15)$$

where

$$K_{tmL} = K_{cL} + C_{slL} \qquad (16)$$

With the mathematic models of EHLS and actuator systems, we can get their relationship in Fig.2.
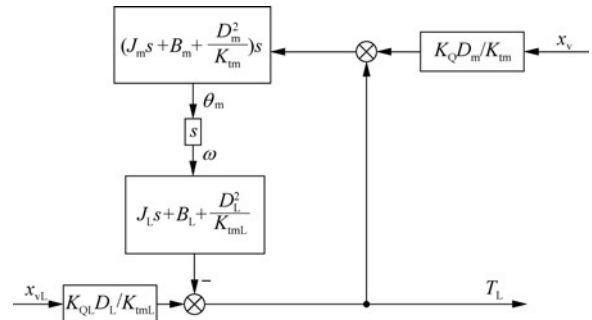

Fig.2   Mathematical models of EHLS and positioning actuator system.

Fig.2 shows that, angular velocity of the actuator is the root of the disturbance torque. It is because of the disturbance torque that conventional controllers do not yield reasonable performance of EHLS. Therefore, many researchers focus on the velocity compensation. Actually, it is unreasonable to regard disturbance torque caused by actuator's motion as a pure disturbance, because this disturbance torque does not always hold back the loading system from building the desired torque, but maybe helps the loading system to produce the desired torque in some cases. In the final analysis, the minimum tracking error is our expectation in EHLS design.

3. Adaptive Nonlinear Optimal Compensation Control

3.1. Analysis of load control

The transfer function of EHLS shown in Eq.(15) includes two parts. One is the load model as follows:

$$G_L(s) = \frac{T_L(s)}{x_{vL}(s)} = \frac{K_{QL}D_L}{K_{tmL}} \quad (17)$$

where $G_L(s)$ is the open-loop transfer function of loading system.

The other part is the disturbance torque caused by actuator's operation:

$$G_P(s) = \frac{T_L(s)}{\theta(s)} = -(J_L s + B_L + \frac{D_L^2}{K_{tmL}})s \quad (18)$$

where $G_P(s)$ is the open-loop transfer function of disturbance torque.

Conventional closed-loop control method collects the torque output and feedback to eliminate its trace error, in which a feed-forward controller is always designed for measurement delay. In this situation, the control output of closed-loop controller is

$$U_{cl} = G(s)E(s) \quad (19)$$

where U_{cl} is the output of loading system, V; $G(s)$ the transfer function of the controller (such as PID controller); $E(s)$ the trace error.

Considering the feed-forward compensation, the total control output is

$$U_L = U_{cl} + U_c \quad (20)$$

where U_L is the total control output of loading system, V; U_c the control output of feed-forward controller, V.

The previous control strategy adopted the combination of feedback and feed-forward control, in which feed-forward eliminates the torque disturbance as a result of the actuator operation and the feedback is used as improving the performance of loading system.

This article designs an optimal compensator based on the velocity synchronizing control structure. It does not regard eliminating disturbance torque as the control objective, but takes the minimum torque trace error as the control target to improve the tracking performance.

From Eq.(19), the torque track error $E(s)$ converges to zero when the closed-loop controller's output of loading system U_{cl} approaches to zero. So it is easy to design the feed-forward controller taking $U_{cl} \rightarrow 0$ as object based on Eq.(17) and Eq.(18). There are two steps to accomplish the feed-forward controller design: the first one is to choose the feed-forward signal and the second one is to design the feed-forward controller.

According to the velocity synchronizing control structure[1,4], the control signal of servo valve is quite full of actuator information with small noise and delay and the actuator could be considered as an integral unit

at low frequency band if the leakage is neglected. Under these conditions, the command signal of servo valve is approximate as actuator velocity. Taking this signal as feed-forward signal is perfect.

The concept of the proposed control strategy considers the EHLS trace and disturbance problems as a whole issue. It not only deals with the disturbance issue presented by Eq.(18), but also handles the torque trace issue shown in Eq.(17), contrasting to the existing velocity compensation methods which focus on how to eliminate the disturbance torque due to the actuator's operation, the proposed control strategy makes the total trace error of EHLS approximate to zero as the control target. The difference between the proposed control strategy and the velocity compensation methods is how to treat Eq.(18). It can be known that the velocity can also provide the desired torque when the $G_L(s)$ given in Eq.(17) and $G_P(s)$ given in Eq.(18) have the same sign with the desired torque. That is to say, the disturbance torque does not always hold back the loading system from building the desired torque, but maybe helps the loading system to produce the desired torque under some conditions.

On the other hand, electro-hydraulic servo system is a typical nonlinear system with parameter variance such as flow gain coefficient and flow-pressure coefficient. This is the reason why fixed gain compensation control methods could not satisfy the loading performance under all working conditions. In order to design an adaptive nonlinear optimal compensation, the parameters of nonlinear system should be evaluated in real time.

3.2. Nonlinear optimal compensation controller design

From Eq.(2), Eq.(5) and Eq.(8), we can obtain the load pressure of actuator system as follows:

$$p_f = \frac{K_Q x_v - D_m \omega}{K_{tm}} \quad (21)$$

Combining with Eq.(6) yields

$$D_m \frac{K_Q x_v - D_m \omega}{K_{tm}} = J_m \omega s + B_m \omega + T_L \quad (22)$$

Similarly, we can get the load pressure of EHLS based on Eq.(10), Eq.(13) and Eq.(16):

$$p_{fL} = \frac{K_{QL} x_{vL} - D_L \omega}{K_{tmL}} \quad (23)$$

Combining with Eq.(14) yields

$$D_L \frac{K_{QL} x_{vL} - D_L \omega}{K_{tmL}} = J_L \omega s + B_L \omega - T_L \quad (24)$$

Connect Eq.(22) and Eq.(24) as

$$(J_m + J_L)\omega s + (B_m + B_L)\omega = D_m \frac{K_Q x_v - D_m \omega}{K_{tm}} +$$

$$D_L \frac{K_{QL} x_{vL} - D_L \omega}{K_{tmL}} \tag{25}$$

Assume that

$$\beta = \frac{D_L}{D_m} \cdot \frac{K_{tm}}{K_{tmL}} \tag{26}$$

where β is the representation of the difference of these two system actuating mechanisms.

Then Eq.(25) can be simplified as

$$(J_m + J_L) \omega s + (B_m + B_L) \omega =$$

$$\frac{D_m}{K_{tm}} [K_Q x_v - D_m \omega + \beta (K_{QL} x_{vL} - D_L \omega)] \tag{27}$$

Due to the high frequency width, the servo valve could be considered as proportional unit:

$$x_v = K_v U_m \tag{28}$$

$$x_{vL} = K_{vL} U_L \tag{29}$$

where U_m is the control output of actuator system, V; K_v and K_{vL} are the spool position gain of actuator and loading servo valve respectively, m/A.

Then

$$K_Q x_v = K_u U_m \tag{30}$$

$$K_{QL} x_{vL} = K_L U_L \tag{31}$$

where K_u and K_L are the voltage-flow gain of actuator and loading servo valve respectively, $m^3 \cdot s^{-1} \cdot V^{-1}$.

Substituting Eq.(30) and Eq.(31) into Eq.(27) yields

$$K_u U_m + \beta K_L U_L = \frac{(J_m + J_L) \omega s + (B_m + B_L) \omega}{\dfrac{D_m}{K_{tm}}} +$$

$$D_m \omega + \beta D_L \omega \tag{32}$$

Taking $U_{cl} \to 0$ as the optimal objective, we can design the feed-forward compensation of adaptive nonlinear controller. In the ideal situation, the following equation exists:

$$U_L = U_c, \quad U_{cl} \to 0 \tag{33}$$

From Section 3.1, its feed-forward signal is the control output of positioning actuator system, so we design a compensator with optimal compensation coefficient ξ as

$$U_c = \xi U_m \tag{34}$$

In real condition, we could also get the following relation based on Eqs.(33)-(34)

$$U_L = \xi U_m \tag{35}$$

Substitute Eq.(35) into Eq.(32), then

$$(K_u + \beta K_L \xi) U_m = \frac{(J_m + J_L) s + (B_m + B_L)}{\dfrac{D_m}{K_{tm}}} \omega +$$

$$D_m \omega + \beta D_L \omega \tag{36}$$

Define

$$J = J_m + J_L \tag{37}$$

$$B = B_m + B_L \tag{38}$$

where J is the total rotor inertia of actuator and EHLS, kg·m²; B the corresponding viscous damping, N·m·s/rad.

Then we could obtain the optimal compensation coefficient ξ as

$$\xi = \frac{J K_{tm} s + B K_{tm} + D_m^2 + \beta D_m D_L}{\beta D_m K_L U_m} \omega - \frac{K_u}{\beta K_L} \tag{39}$$

The nonlinear optimal compensation controller can be described as

$$U_c = \xi U_m =$$

$$\frac{(J K_{tm} s + B K_{tm} + D_m^2 + \beta D_m D_L) \omega - D_m K_u U_m}{\beta D_m K_L} \tag{40}$$

It is obvious that the compensator contains both the unit of loading system and one of positioning actuator systems, so it is more comprehensive to improve the performance of EHLS.

Note that the above derivations could extend to any other complicated conditions as long as $U_{cl} \to 0$. And the assumption can be achieved as long as the nonlinear optimal compensator is designed reasonably and effectively, then the closed-loop controller's output of the loading system would always maintain low level. This is to say, the assumption of the proposed control strategy basically holds true. Due to the control signal coming from the positioning actuator, only the optimal compensation could not achieve the ideal performance of torque track, and it must be combined with other closed-loop controller. At the same time, it is clear that the compensation unit contains nonlinear and varying parameters shown in Eq.(40). So it is necessary to evaluate the parameters to construct the adaptive compensator.

3.3. Online estimation of nonlinear parameters

Hydraulic servo systems are highly nonlinear system. The main nonlinear parameters are flow gain coefficient and flow pressure coefficient. From Eq.(26), Eqs.(30)-(31) and Eqs.(37)-(39), the optimal compensation coefficient ξ contains static parameters as J_m, J_L, B_m, B_L, D_m, D_L and dynamic parameters as K_u, K_L, K_{tm}, K_{tmL}. In order to improve the dynamic performance, the update dynamic parameters should be used in adaptive nonlinear optimal compensation design.

With Eq.(21) and Eq.(23), we can get

$$K_{tm} = \frac{K_Q x_v - D_m \omega}{p_f} \tag{41}$$

$$K_{tmL} = \frac{K_{QL} x_{vL} - D_L \omega}{p_{fL}} \tag{42}$$

Based on Eq.(6) and Eq.(14), we can obtain

$$p_f = \frac{J_m \omega s + B_m \omega - T_L}{D_m} \tag{43}$$

$$p_{fL} = \frac{J_L \omega s + B_L \omega + T_L}{D_L} \tag{44}$$

Then,

$$K_{tm} = \frac{(K_Q x_v - D_m \omega) D_m}{J_m \omega s + B_m \omega - T_L} \tag{45}$$

$$K_{tmL} = \frac{(K_{QL} x_{vL} - D_L \omega) D_L}{J_L \omega s + B_L \omega + T_L} \tag{46}$$

Combining Eq.(30) and Eq.(31), then

$$K_{tm} = \frac{(K_u U_m - D_m \omega) D_m}{J_m \omega s + B_m \omega - T_L} \tag{47}$$

$$K_{tmL} = \frac{(K_L U_L - D_L \omega) D_L}{J_L \omega s + B_L \omega + T_L} \tag{48}$$

From Eq.(1), servo valve idle flow Q_o can be described as

$$Q_o = C_v W x_{vmax} \sqrt{\frac{1}{\rho} p_s} \tag{49}$$

Substituting Eq.(28) into Eq.(49) yields

$$Q_o = C_v W K_v U_{max} \sqrt{\frac{1}{\rho} p_s} \tag{50}$$

So,

$$C_v W K_v \sqrt{\frac{1}{\rho}} = \frac{Q_o}{U_{max} \sqrt{p_s}} \tag{51}$$

Define

$$K_{to} = C_v W K_v \sqrt{\frac{1}{\rho}} = \frac{Q_o}{U_{max} \sqrt{p_s}} \tag{52}$$

Simultaneously, substituting Eq.(28) into Eq.(30) yields

$$K_u = K_v K_Q = K_v C_v W \sqrt{\frac{1}{\rho}} \cdot \sqrt{p_s - \text{sign}(U_m) p_f} \tag{53}$$

So,

$$K_u = K_{to} \sqrt{p_s - \text{sign}(U_m) p_f} \tag{54}$$

In a similar way, the following equation can be got

$$K_L = K_{toL} \sqrt{p_{sL} - \text{sign}(U_L) p_{fL}} \tag{55}$$

where

$$K_{toL} = C_{vL} W_L K_{vL} \sqrt{\frac{1}{\rho}} = \frac{Q_{oL}}{U_{Lmax} \sqrt{p_{sL}}} \tag{56}$$

3.4. Adaptive nonlinear optimal compensation control strategy

The scheme of the adaptive nonlinear optimal compensation control strategy is illustrated in Fig.3. It is obvious that the individual actuator and EHLS adopt the PID controller and the interconnection utilizes the adaptive nonlinear optimal compensator in which the control signal of servo valve in actuator system is introduced. The interconnection compensator exploits updatable nonlinear parameters in real time to compensate the motion disturbance to achieve optimal performance with the controller shown in Section 3.3.

The controller acquires data from torque sensor and angular sensor and further acquires the velocity and acceleration signal by a three-order derivative algorithm, then combines with the control output of the actuator to calculate the controller's output. The proposed compensator contains more information of the loading system and the actuator system, so it can make more precise control to improve the performance of the EHLS. Due to the nonlinear parameter estimation, the compensator can acclimatize itself to all working conditions. And so this compensator can provide the satisfactory trace performance operating in any working conditions.
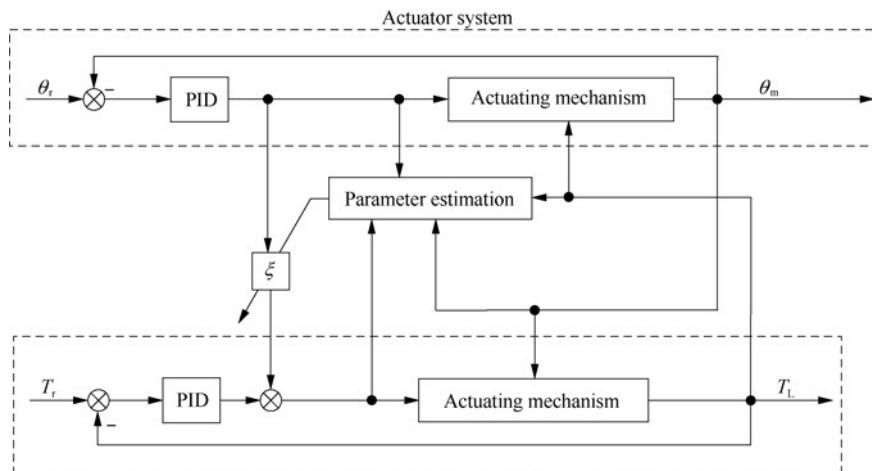

Fig.3   Adaptive nonlinear optimal compensation control scheme.

4. Case Study

4.1. Experimental test rig configuration

The experimental platform is shown in Fig.4. This platform consists of bench case, load channels (including hydraulic rotary actuator, torque sensor, angular encoder, servo valve and shaft joint, etc.), hydraulic supply, measurement and control system (MACSYM). All load channels are completely the same. In Fig.4, the left part acts as the loading system, i.e. EHLS, and the right one acts as the positioning actuator system which is used to produce the motion disturbance. That is to say that the loading system will be used to verify the proposed control strategy designed for EHLS, and the actuator system is only controlled by the positioning closed-loop PID control. Table 1 shows the parameters in details of the main components.

The measurement and control system consists of monitoring software and real time control software. The monitor software is programmed with NI Lab-Windows/CVI and the real time control software is compiled with Microsoft Visual Studio 2005 plus Ardence RTX 7.0. Ardence RTX 7.0 is used to provide the real time working environment for the real time control software under the Windows XP operating system. The real time control software's sampling time is 0.5 ms. The test computer is the IEI WS-855GS. A/D and D/A transfer boards are Advantech PCI-1716 and Advantech PCI-1723. The angular encoder used in MACSYM is Renishaw RGH20. The actuators of this test rig are designed and manufactured by our hydraulic laboratory. And hydraulic servo valve is Moog G761-3005.
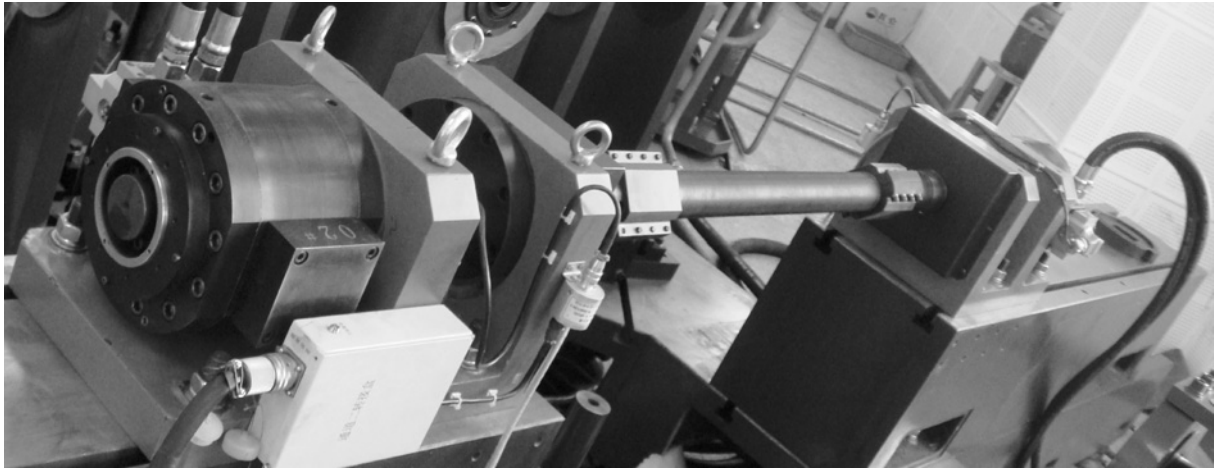

Fig.4 EHLS test rig.

Table 1 Specification of EHLS and actuator system

Component	Specification	
Hydraulic supply	Number	2
	System pressure	21 MPa
	Max continuous flow rate	120 L/min
Servo valve	Number	2
	Type	Moog G761-3005
	Rated flow	63 L/min
Hydraulic actuator	Number	2
	Angular range	−35°-35°
	Radian displacement	0.191 67 L/rad
	Stall torque	2 300 N·m
Torque sensor	Number	2
	Range	−2 800-2 800 N·m
	Accuracy	0.3%
Angular sensor	Number	2
	Type	Renishaw RGH20
	Accuracy	20″
A/D card	Type	Advantech PCI-1716
D/A card	Type	Advantech PCI-1723
Counter	Type	NI PCI-6601
Computer	Type	IEI WS-855GS

The static parameters of loading and actuator system are given as follows:

$$\begin{cases} J=0.078\ 58\ \text{kg}\cdot\text{m}^2 \\ B_m=B_L=45\ \text{N}\cdot\text{m}\cdot\text{s/rad} \\ D_m=D_L=0.191\ 67\ \text{L/rad} \\ K_{to}=K_{to}L=3.968\ 63\times10^{-8} \end{cases}$$

Because the designed adaptive nonlinear optimal compensation control is based on the systems' models, it is necessary to ensure the validity of the system models and estimation of system dynamic parameters firstly. And then it can be ensure that the adaptive nonlinear optimal compensation control is reasonable and valid.

4.2. Validity demonstration

From the system model, we could deduce the output of loading system in reverse if the compensator design is reasonable and the estimation of system dynamic parameters is exact enough. That could validate the effectiveness of adaptive nonlinear optimal compensator.

From Eq.(32), we could get the output of loading

system as

$$U_{\mathrm{L}} = \frac{(JK_{\mathrm{tm}}s + BK_{\mathrm{tm}} + D_{\mathrm{m}}^2 + \beta D_{\mathrm{m}}D_{\mathrm{L}})\omega - D_{\mathrm{m}}K_{\mathrm{u}}U_{\mathrm{m}}}{\beta D_{\mathrm{m}}K_{\mathrm{L}}}$$

(57)

Comparing Eq.(57) with Eq.(40), it is obvious that the two expressions are uniform. The control output calculated by the adaptive nonlinear optimal compensation is just the total control output of the loading servo system. It is intelligible because the design law of the adaptive nonlinear optimal compensation controller is to make the torque closed-loop control output converge to zero. So the control output of the adaptive nonlinear optimal compensation controller is precisely approximate to the total output of loading system in the ideal situation. Moreover, the total control output of the loading system equals the control output of torque closed-loop controller before the control output of the adaptive nonlinear optimal compensation controller is incorporated into the total control output. Thus, it indicates that the adaptive nonlinear optimal compensation controller is reasonable and the estimation of system nonlinear parameters is accurate, if the control output of adaptive nonlinear optimal compensation controller is sufficiently close to the output of torque closed-loop controller.

In essence, the adaptive nonlinear optimal compensation controller is a kind of torque holder that could maintain the current output torque. That means the task of adaptive nonlinear optimal compensation controller is in charge of maintaining output torque while the torque controller is responsible for the torque trace based on update torque. Meanwhile, there is a clear function division between adaptive nonlinear optimal compensation controller and torque closed-loop controller. The former betakes to maintain torque output and the latter is responsible for torque updating.

Considering the acquisition error and external disturbance, it is necessary to design a filter that could eliminate these disturbances. This article adopts a second-order Butterworth filter whose cutoff frequency is 50 Hz and sampling period is 0.5 ms. Its transfer function is given as:

$$G_{\mathrm{filter}} = \frac{0.005\,521z^{-2} + 0.011\,04z^{-1} + 0.005\,521}{0.801\,2z^{-2} - 1.779z^{-1} + 1}$$

(58)

The demonstration experiment is carried out on the test rig shown in Fig.4. The estimation result is given in Fig.5 which indicates that the control output of the adaptive nonlinear optimal compensation controller is close to the control output of torque closed-loop controller when actuator sinuous input's amplitude is 5° and frequency is 2 Hz, and loading system sinuous input's amplitude is 1 000 N·m and frequency is 1 Hz. The real control curve is the representation of the control output of torque closed-loop controller and the estimation control curve is the representation of the output of the adaptive nonlinear optimal compensation controller in Fig.5(a). Fig.5(b) is the estimation error

between real control curve and estimation control curve. The estimation result after filter is presented in Fig.5(c).
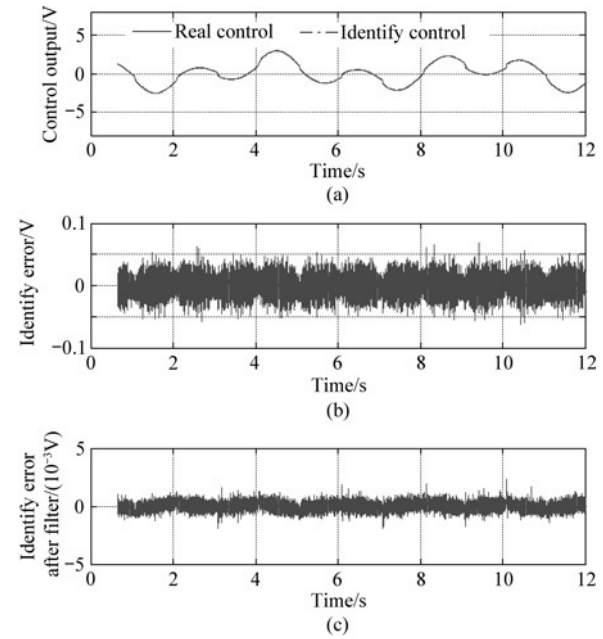

Fig.5 Estimation of adaptive nonlinear optimal compensation control (1).

The demonstration experiment under another reference command is shown in Fig.6. The actuator tracks sinuous input signal whose amplitude is 10° and frequency is 0.5 Hz, and loading system tracks sinuous input signal whose amplitude is 500 N·m and frequency is 0.2 Hz in this experiment. It is seen that the maximum estimation error is close to 0.005 V after filter in Fig.6(c). These two estimation experiments show that the maximum estimation error is no more than 0.2% of the maximum control output.
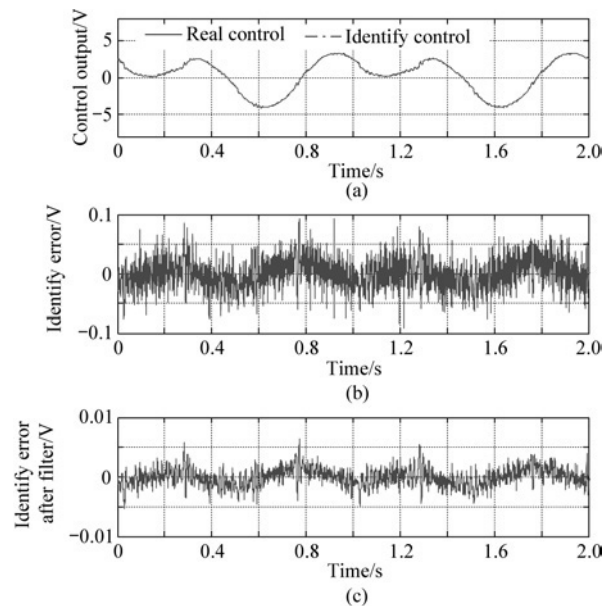

Fig.6 Estimation of adaptive nonlinear optimal compensation control (2).

4.3. Torque tracking performance under various typical working conditions

To verify the ability of the proposed adaptive nonlinear optimal compensation control, this article sets up abundant experiments over a wide range of typical working conditions which are normally used to test and appraise the actuator's system, that is to say these typical working conditions can indicate the EHLS main performance. These typical working conditions mainly contain three cases: 1) static loading; 2) gradient loading, including positive gradient and negative gradient; 3) arbitrary amplitude loading at different frequencies between EHLS and positioning actuator system. Static loading condition can present the tracing performance of EHLS itself without actuator motion disturbance. This condition can test the actuator's static rigidity. Gradient loading condition can present the EHLS synthetical abilities to trace target torque with various actuator motion disturbances at the same frequency. This condition is the most common test type for actuator system. Arbitrary loading condition can present the EHLS' ability of tracing random loading target under arbitrary motion disturbances. These three typical cases include all the required EHLS performance. And to verify the tracking performance, three control strategies are employed to compare the experimental results. The first one is non-compensation strategy, it means that, loading system only applies conventional PID controller; the second is velocity synchronizing control[1,4] added by PID controller; and the last one is the proposed adaptive nonlinear optimal compensation control joining with PID controller. All PID controllers have the same tuning parameters.

Define the loading gradient[20]: when the displacement is positive and the actuator is moving to positive direction, the loading torque is resistance for actuator's moving, the loading gradient is positive; vice versa.

(1) Static loading experiment

In this experiment, positioning servo system conducts zero command tracking and EHLS, designated torque tracking. This experiment is to investigate the tracking performance without velocity disturbance. Fig.7 denotes the comparison of the three control strategies under tracking sinuous torque input whose amplitude is 1 500 N·m and frequency is 1 Hz. This result shows the maximum trace errors are approximately 120, 200 and 18 N·m achieved by PID control, velocity synchronizing control and the proposed control respectively. It is seen that the proposed control strategy's trace accuracy reaches almost 99%, comparable to 92% and 86.6% of the trace accuracy achieved by PID control and velocity synchronizing control respectively. This experiment shows that under the same conditions, the proposed algorithm can increase trace accuracy by 7% and 12.4%, compared with the existing PID control and velocity synchronizing control respectively. This experiment also indicates that the velocity synchronizing control method is even

(a) No compensation, only PID control

(b) Velocity synchronizing control plus PID control

(c) Adaptive nonlinear optimal compensation control plus PID control
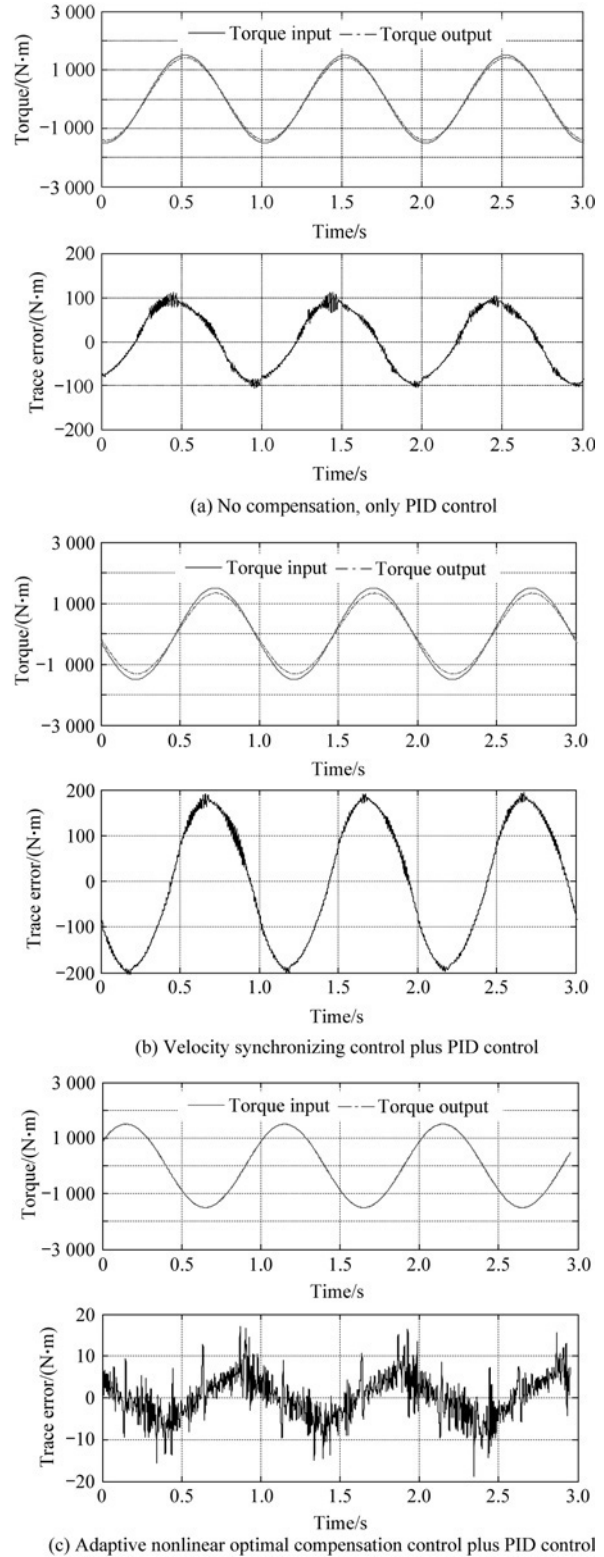
Fig.7   Comparison of three control strategies under tracking sinuous torque input in static loading situation.

worse than the only PID control due to the concept of the velocity synchronizing control providing wholly opposite control direction under static working conditions.

(2) Gradient loading experiment

Gradient loading is the experiment that the loading

torque command is proportional to the actuator's position command. It can be divided into four loading cases which are large load tracking with high-speed disturbance, small load tracking with high-speed disturbance, large load tracking with low-speed disturbance, small load tracking with low-speed disturbance respectively. And the loading gradient can be positive or negative.

Fig.8 shows that the comparison among three control strategies with the large torque tracking with high-speed disturbance operating condition. Positioning servo system plays sine movement of 10° amplitude and 2 Hz and the loading system tracking gradient is 200 N·m/(°) in this test. This result displays the maximum trace errors are approximately 250, 245 and 50 N·m achieved by PID control, velocity synchronizing control and the proposed adaptive nonlinear optimal compensation control respectively. It is seen that the nonlinear characteristic of hydraulic servo system is very critical when large load couples with high-speed disturbance. The nonlinear characteristic will cause fixed gains controller or compensator does not to yield reasonable performance. Hence, the proposed controller which has adaptive property can achieve better tracking performance than the other two control strategies. It is seen that the proposed control strategy's trace accuracy
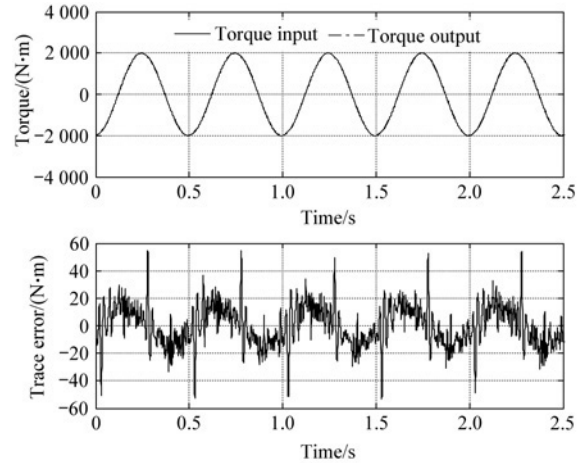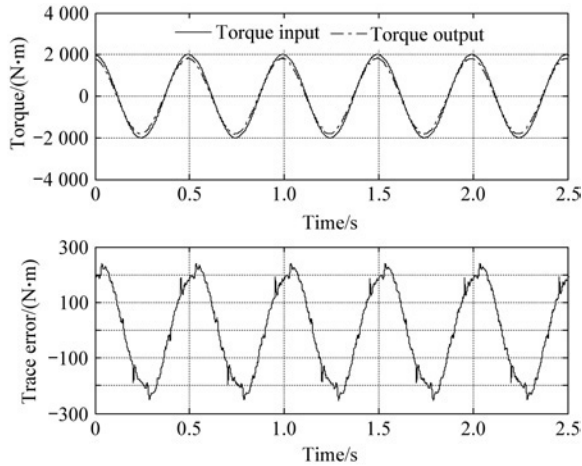

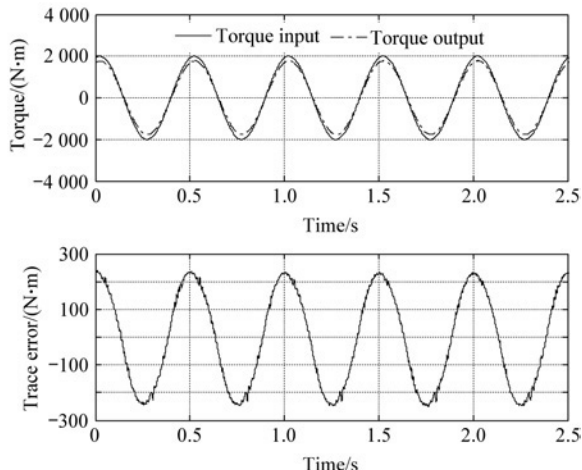(c) Adaptive nonlinear optimal compensation control plus PID control

Fig.8   Comparison of three control strategies under loading gradient in large load with high-speed disturbance situation.

reaches almost 97.5%, comparable to 87.5% and 87.7% of the trace accuracy achieved by PID control and velocity synchronizing control respectively. Under the harsh working conditions, the velocity synchronizing control method almost achieves the same trace accuracy as the only PID control method. That means the velocity synchronizing control method hardly works. Experimental results show that under the same positive gradient conditions which are the large torque tracking with high-speed disturbance operating condition, the proposed algorithm can increase trace accuracy by 10%, compared with the existing PID control and velocity synchronizing control methods.
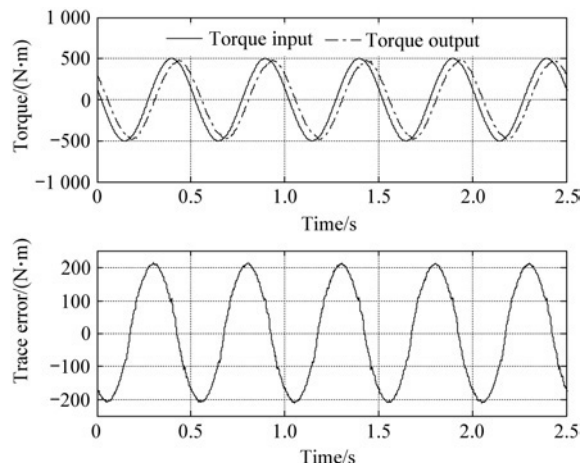
The experimental results of three control strategies under the small load tracking with high-speed disturbance situation are given in Fig.9. In this case, positioning servo system plays sine movement of 10° amplitude and 2 Hz and the loading system tracking gradient is −50 N·m/(°). The maximum trace error of about 25 N·m is achieved by adaptive nonlinear optimal compensation control, comparable to 210 N·m and 92 N·m of the maximum trace error achieved by PID

(a) No compensation, only PID control

(b) Velocity synchronizing control plus PID control

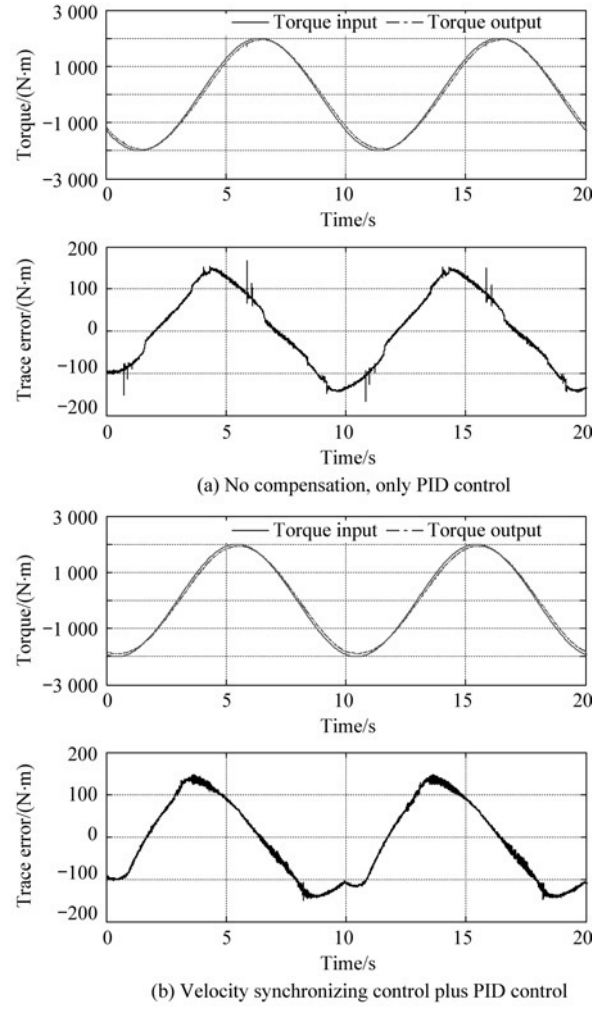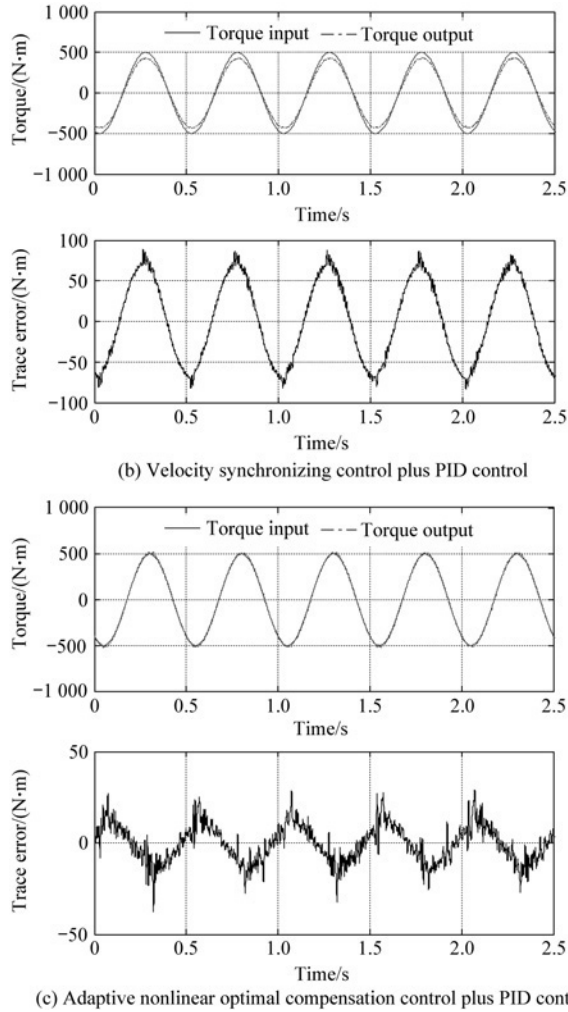(a) No compensation, only PID control

(b) Velocity synchronizing control plus PID control

(c) Adaptive nonlinear optimal compensation control plus PID control

Fig.9   Comparison of three control strategies under loading gradient in small load with high-speed disturbance situation.

(a) No compensation, only PID control

(b) Velocity synchronizing control plus PID control

(c) Adaptive nonlinear optimal compensation control plus PID control

Fig.10   Comparison of three control strategies under loading gradient in large load with low-speed disturbance situation.

control and velocity synchronizing control respectively. It can be known that the proposed control strategy's trace accuracy reaches almost 95%, while the PID control method and the velocity synchronizing control method can reach 58% and 82% of the trace accuracy respectively. Experimental results show that under the same negative gradient conditions, i.e., small load tracking with high-speed disturbance operating situation, the proposed algorithm can increase trace accuracy by 36% and 12%, compared with the existing PID control and velocity synchronizing control methods.

Fig.10 presents the experimental results of the three control strategies based on large load tracking with low-speed disturbance situation. And the positioning servo system plays sine movement of 5° amplitude and 0.1 Hz frequency and the loading system tracking gradient is −400 N·m/(°). The maximum trace error of about 15 N·m is achieved by the proposed control, comparable to 150 N·m and 145 N·m of the trace accuracy achieved by PID control and velocity synchronizing control respectively. The proposed algorithm can increase trace accuracy by almost 7%, compared with the existing control methods.
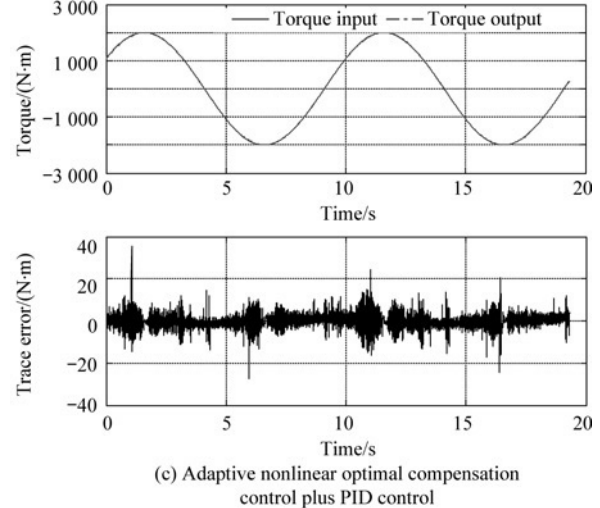
Finally, the experimental results of three control strategies under the small load tracking with low-speed disturbance situation are illustrated in Fig.11. Positioning servo system plays sine movement of 5° amplitude and 1 Hz frequency and loading system tracking gradient is −100 N·m/(°). The maximum trace error about 10 N·m is achieved by the proposed

about 10 N·m is achieved by the proposed control, comparable to 110 N·m and 70 N·m achieved by PID control and velocity synchronizing control respectively. The proposed algorithm can increase trace accuracy by 20% and 12%, compared with the existing control methods.
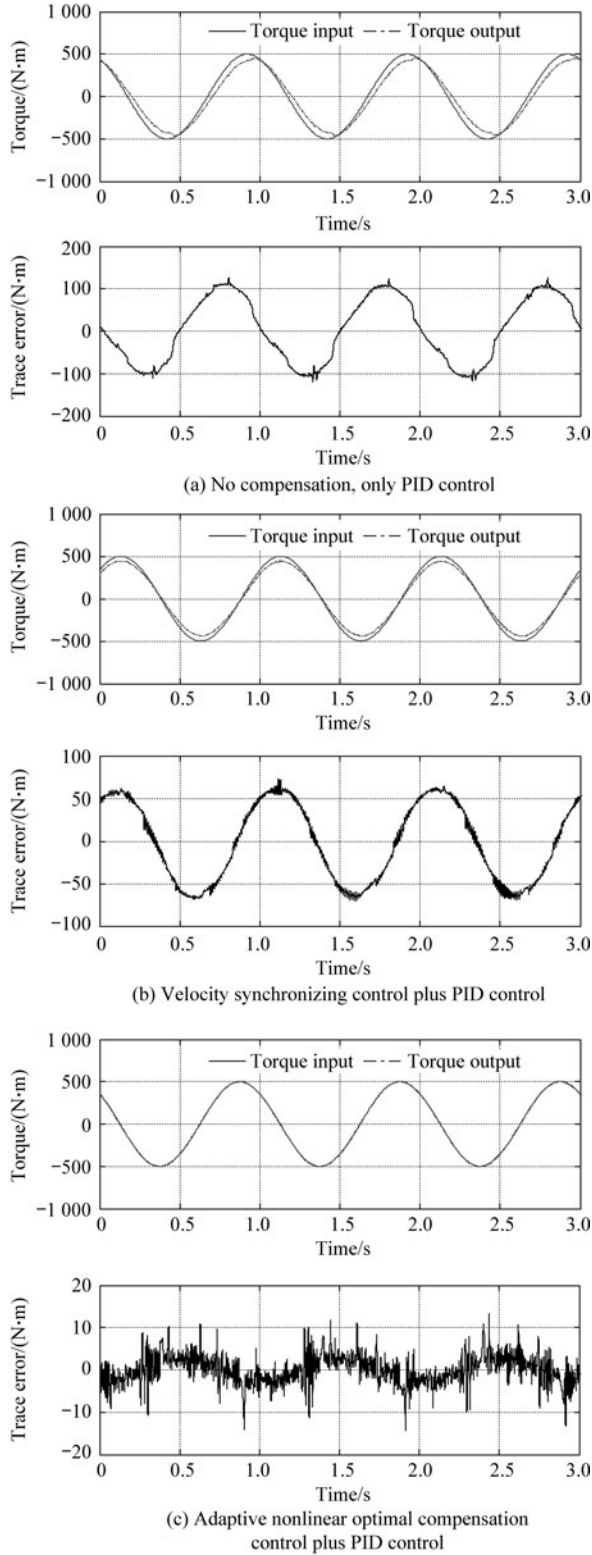
(3) Arbitrary loading at different frequencies

In order to further validate the control strategy, this article performs the experiment of different frequencies, making actuator and loading system follow their commands at different frequencies.

The tracking results of three control strategies are shown in Fig.12. The loading system and the actuator

(a) No compensation, only PID control

(b) Velocity synchronizing control plus PID control

(c) Adaptive nonlinear optimal compensation control plus PID control

Fig.11   Comparison of three control strategies under loading gradient in small load with low-speed disturbance situation.

(a) No compensation, only PID control

(b) Velocity synchronizing control plus PID control

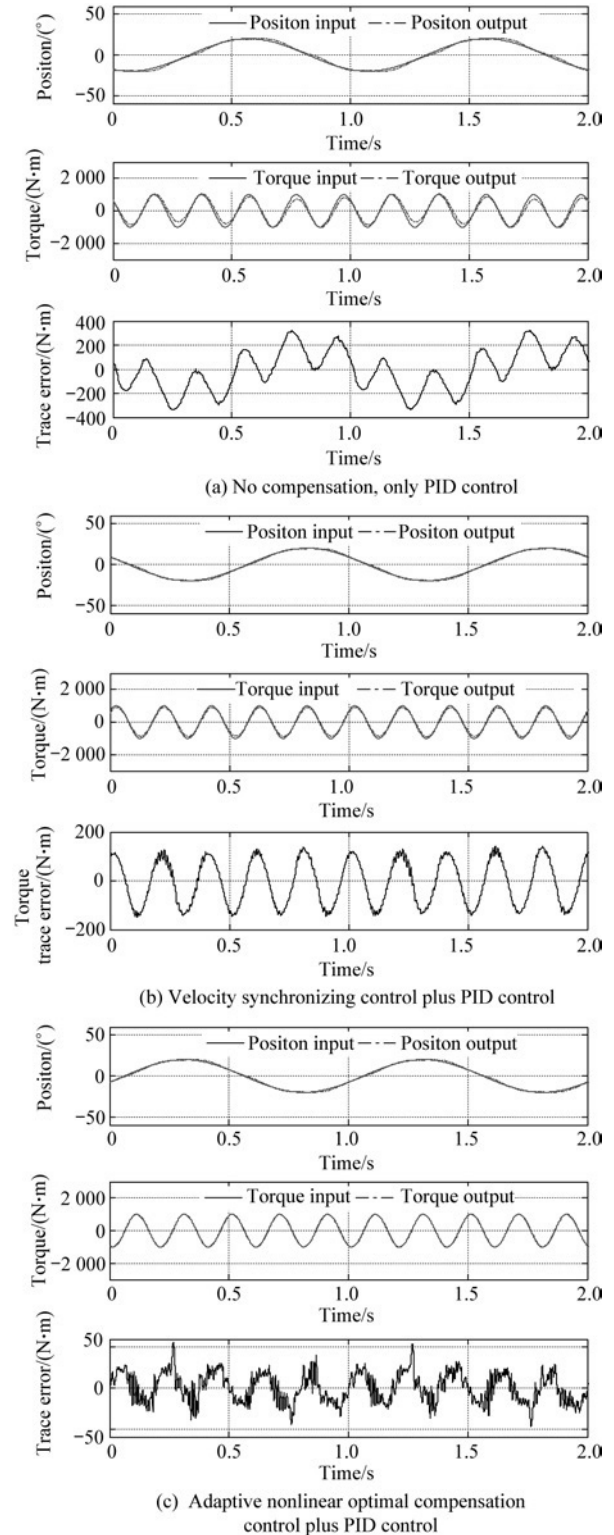(c) Adaptive nonlinear optimal compensation control plus PID control

Fig.12   Comparison of three control strategies under proportional tracing, low speed and little load.

system play sine commands at different frequencies.

Positioning servo system plays sine movement of 20° amplitude and 1 Hz frequency, with loading system tracking sine torque of 1 000 N·m amplitude and frequency of 5 Hz in this experiment. As a result, the maximum tracking error of about 50 N·m is achieved by adaptive nonlinear optimal compensation control. While the maximum tracking error of about 150 N·m is given by velocity synchronizing control strategy, the tracking is almost unstable when the conventional PID controller is adopted only. The proposed algorithm can increase trace accuracy by 10% compared with the existing velocity synchronizing control strategy methods.

Fig.13 gives the controller's output data of the arbitrary loading experiment shown in Fig.12. The first graph contains two curves: the total controller's output of the loading system and the output of the proposed adaptive nonlinear optimal compensation controller. The second one indicates the error curve between the total controller's output and the proposed controller. It can be seen that the error curve is also the PID controller's output from the proposed control scheme shown in Fig.3.
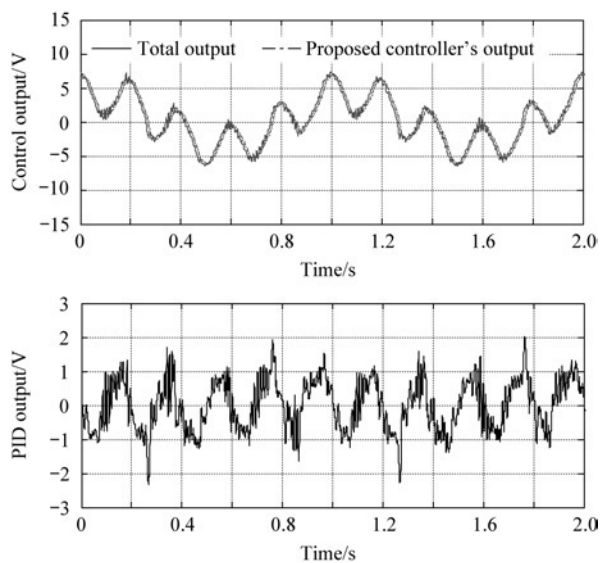

Fig.13 Controller's output of loading system in arbitrary loading experiment.

It is known from Fig.13 that the proposed controller's output is the main part of the total control output of the loading system, and the PID controller's output maintains a low level, which is used to resist the outer and/or inner disturbance. That is to say, the PID controller's control output is less than 30% of the total control output.

5. Conclusions

An adaptive nonlinear optimal compensation controller has been designed and nonlinear parameter estimation has been done in this article, which is aimed at improving the torque tracking performance of electro-hydraulic load simulator. It has the following characteristics:

(1) The concept of the proposed adaptive nonlinear optimal compensation control is different from previous control concepts. Its objective is to make the control output of torque closed-loop controller converge to zero. Meantime, online estimation system nonlinear parameters adapt to the optimal compensator because of the nonlinear characteristic of hydraulic system, and the maximum estimation error of control output is no more than 0.2% of the maximum control output.

(2) It satisfies the tracking performance under various operating conditions. A large number of experiments show that the adaptive nonlinear optimal compensation controller is adequate for the loading demands under various working conditions which contain static loading without velocity disturbance, gradient loading with various velocity disturbances and load tracking with different frequencies. The proposed control strategy maintains 95% or greater trace accuracy under all typical working conditions, while the existing velocity synchronizing control strategy can be used very well only under zero torque command trace. Its performance fluctuation is large, with accuracy ranging from 80% to 95% under different working conditions. The only PID control method's performance fluctuation is very large than the velocity synchronizing control strategy, even tends to be in an unstable state under some working conditions.

(3) It reduces the burden of the torque closed-loop controller and provides a sufficient margin for the torque closed-loop controller to respond to varieties of burst interference. The PID controller's control output is less than 30% of the total control output when using the proposed control strategy under arbitrary loading.

Acknowledgment

References

[1]	Hua Q. Studies on the key technology of electro-hydraulic load simulator. PhD thesis, School of Automation Science and Electric Engineering, Beijing University of Aeronautics and Astronautics, 2001. [in Chinese]

[2]	Liu C N. The optimized design theory of hydraulic servo system. Beijing: Metallurgical Industry Press, 1989. [in Chinese]

[3]	Yu C Y, Liu Q H, Zhao K D. Velocity feedback in load simulator with a motor synchronizing in position. Journal of Harbin Institute of Technology: New Series 1998; 5(3): 78-81.

[4]	Jiao Z X, Gao J X, Hua Q, et al. The velocity synchronizing control on the electro-hydraulic load simulator. Chinese Journal of Aeronautics 2004; 17(1): 39-46.

[5]   Wang X, Sun L, Yan J. Experimental research on im-
       proving loading performance by compounding feed-
       forward control. Journal of System Simulations 2004;
       16(7): 1539-1541. [in Chinese]

[6]   Yao J Y, Shang Y X, Jiao Z X. The velocity
       feed-forward and compensation on eliminating extra-
       neous torque of electro-hydraulic load simulator. Pro-
       ceedings of the seventh international conference on
       fluid power transmission and control. 2009; 462-465.

[7]   Plummer A R. Control techniques for structural test-
       ing: a review. Proceedings of the Institution of Me-
       chanical Engineers, Part I: Journal of Systems and
       Control Engineering 2007; 221(12): 139-170.

[8]   Truong D Q, Ahn K K. Force control for hydraulic
       load simulator using self-tuning grey predictor – fuzzy
       PID. Mechatronics 2009; 19(2): 233-246.

[9]   Plummer A R. Robust electro-hydraulic force control.
       Proceedings of the Institution of Mechanical Engi-
       neers, Part I: Journal of Systems and Control Engi-
       neering 2007; 221(2): 717-731.

[10]   Yoonsu N, Sung K H. Force control system design for
       aerodynamic load simulator. Control Engineering
       Practice 2002; 10(5): 549-558.

[11]   Yoonsu N. QFT force loop design for the aerodynamic
       load simulator. IEEE Transaction on Aerospace and
       Electronic Systems 2001; 37(4): 1384-1392.

[12]   Mare F C. Dynamic loading systems for ground testing
       of high speed aerospace actuators. Aircraft Engineering
       and Aerospace Technology: an international Journal
       2006; 78(4): 275-282.

[13]   Chantranuwathana S, Peng H. Adaptive robust force
       control for vehicle active suspensions. International
       Journal of Adaptive Control and Signal Processing
       2004; 18(2): 83-102.

[14]   Jiao Z X, Hua Q. RBF neural network control on elec-
       tro-hydraulic load simulator. Chinese Journal of Me-
       chanical Engineering 2003; 39(1): 10-14. [in Chinese]

[15]   Wang X M, Liu W G. Neural network internal feed-
       back control for electro-hydraulic servo loading. Acta
       Aeronautica et Astronautica Sinica 2007; 28(3):
       690-694. [in Chinese]

[16]   Zhang B, Zhao K D, Sun F Y. Neural network pa-
       rameter identification of electro-hydraulic load simu-
       lator. Acta Aeronautica et Astronautica Sinica 2009;
       30(2): 374-379. [in Chinese]

[17]   Liu G P, Daley S. Optimal-tuning nonlinear PID con-
       trol of hydraulic systems. Control Engineering Practice
       2000; 8(9): 1045-1053.

[18]   Liu G P, Daley S. Optimal-tuning PID control for in-
       dustrial systems. Control Engineering Practice 2001;
       9(11): 1185-1194.

[19]   Abbott R D, McLain T W, Beard R W. Application of
       an optimal control synthesis strategy to an elec-
       tro-hydraulic positioning system. ASME Journal of
       Dynamic Systems, Measurement, and Control 2001;
       123(3): 377-384.

[20]   Shang Y X. Study on ultimate performance of elec-
       tro-hydraulic load simulator. PhD thesis, School of
       Automation Science and Electric Engineering, Beijing
       University of Aeronautics and Astronautics, 2009. [in
       Chinese]

Biographies:

Yao Jianyong   Born in 1984, he received B.S. degree from
Tianjin University in 2006 and now is a Ph.D. candidate in
School of Automation Science and Electric Engineering,
Beijing University of Aeronautics and Astronautics. His
main research interests lie in hydraulic servo control, mecha-
tronics and hardware in the loop simulation.
E-mail: jerryyao.buaa@gmail.com

Jiao Zongxia   Born in 1963, Professor, Ph.D., president of
School of Automation Science and Electric Engineering,
Beijing University of Aeronautics and Astronautics. His
main research interests are fluid power transmission and
control, mechatronics systems, simulation engineering.
E-mail: zxjiao@buaa.edu.cn